

# 1 **Exact solutions of linear reaction-diffusion processes** 2 **on a uniformly growing domain: Criteria for** 3 **successful colonization**

4 Matthew J Simpson<sup>1,\*</sup>

5 **1 Mathematical Sciences, Queensland University of Technology, Brisbane,**  
6 **Australia.**

7 \* **E-mail: [matthew.simpson@qut.edu.au](mailto:matthew.simpson@qut.edu.au)**

## 8 **Abstract**

9 Many processes during embryonic development involve transport and reaction of molecules,  
10 or transport and proliferation of cells, within growing tissues. Mathematical models of  
11 such processes usually take the form of a reaction–diffusion partial differential equation  
12 (PDE) on a growing domain. Previous analyses of such models have mainly involved solv-  
13 ing the PDEs numerically. Here, we present a framework for calculating the exact solution  
14 of a linear reaction–diffusion PDE on a growing domain. We derive an exact solution for  
15 a general class of one–dimensional linear reaction–diffusion process on  $0 \leq x \leq L(t)$ ,  
16 where  $L(t)$  is the length of the growing domain. Comparing our exact solutions with  
17 numerical approximations confirms the accuracy of the method. Furthermore, our exam-  
18 ples illustrate a delicate interplay between: (i) the rate at which the domain elongates,  
19 (ii) the diffusivity associated with the spreading density profile, (iii) the reaction rate,  
20 and (iv) the initial condition. Altering the balance between these four features leads to  
21 different outcomes in terms of whether an initial profile, located near  $x = 0$ , eventually  
22 overcomes the domain growth and colonizes the entire length of the domain by reaching  
23 the boundary where  $x = L(t)$ .

## 24 **Introduction**

25 Developmental processes are often associated with transport and reaction of molecules,  
26 or transport and proliferation of cells, within growing tissues [1, 2]. For example, the de-  
27 velopment of biological patterns, such as animal coat markings, is thought to arise due to  
28 the coupling between an activator-inhibitor Turing mechanism and additional transport  
29 induced by tissue growth [3–7]. Within the mathematical biology literature, there is an  
30 increasing awareness of the importance of incorporating domain growth into mathemat-  
31 ical models of various biological processes including morphogen gradient formation [8]  
32 and models of collective cell spreading [9]. In addition to considering particular bio-  
33 logical applications, other studies have focused on examining more theoretical questions  
34 associated with reactive transport processes on growing domains. Most notably, several  
35 previous studies have examined the relationship between discrete random walk models  
36 and associated continuum partial differential equation (PDE) descriptions [10–14].

37 One particular biological application where transport and reaction (proliferation) of  
38 cells takes place on a growing domain is the development of the enteric nervous system  
39 (ENS) [15–21]. This developmental process involves neural crest precursor cells entering  
40 the oral end of the developing gut. Individual precursor cells migrate and proliferate,  
41 which results in the formation of a moving front of precursor cells which travels towards  
42 the anal end of the developing gut. This colonization process is complicated by the  
43 fact that the gut tissues elongate simultaneously as the cell front moves [17]. Normal  
44 development requires that the moving front of precursor cells reaches the anal end of  
45 the developing tissue. Abnormal development is thought to be associated with situations  
46 where the moving front of cells fails to completely colonize the growing gut tissue [17].

47 One of the first mathematical models of ENS development, described by Landman

48 et al. [22], is a PDE description of the migration and proliferation of a population of  
49 precursor cells on a uniformly growing tissue. In particular, Landman et al. [22] use  
50 their model to mimic ENS development by considering an initial condition where the  
51 population of precursor cells is initially confined towards one end of the domain. Landman  
52 et al. [22] solve the governing PDE numerically and use these numerical solutions to  
53 explore whether the population of cells can colonize the entire length of the growing  
54 domain within a certain period of time. In particular, Landman et al. [22] highlights an  
55 important interaction between: (i) the initial distribution of cells; (ii) the migration rate  
56 of cells; (iii) the proliferation rate of cells; and (iv) the growth rate of the underlying  
57 tissue. Landman et al. [22] explore the relationship between these four factors using an  
58 approximate numerical solution of the PDE model. These previous numerical results  
59 suggest that successful colonization requires: (i) that the initial length of colonization  
60 must be sufficiently large, (ii) that the migration rate of cells is sufficiently large, (iii)  
61 that the proliferation rate of cells is sufficiently large, and (iv) that the growth rate of the  
62 underlying tissue is sufficiently small.

63 The focus of the present work is to consider a linear reaction-diffusion process on a  
64 growing domain with a view to obtaining an exact solution of the associated PDE. After  
65 transforming the PDE to a fixed domain we obtain a PDE with variable coefficients. The  
66 variable coefficient PDE is simplified using an appropriate transformation which enables us  
67 to obtain an exact solution using separation of variables. While our strategy for obtaining  
68 an exact solution is quite general, we present specific results for linear and exponentially  
69 elongating domains. After verifying the accuracy of our exact solutions using numerical  
70 approximations, we summarise our results in terms of a concise condition that can be used  
71 to distinguish between successful or unsuccessful colonization. We conclude this study by  
72 acknowledging the limitations of our analysis, and we outline some further extensions of

73 our approach which could be implemented in future studies.

## 74 1 Materials and methods

### 75 1.1 Mathematical model

76 We consider a linear reaction-diffusion process on a one-dimensional domain,  $0 \leq x \leq L(t)$ ,  
77 where  $L(t)$  is the increasing length of the domain. Domain growth is associated with a  
78 velocity field which causes a point at location  $x$  to move to  $x + v(x, t)\tau$  during a small  
79 time period of duration  $\tau$  [22]. By considering the expansion of an element of initial width  
80  $\Delta x$ , we can derive an expression relating  $L(t)$  and  $v(x, t)$ , which can be written as

$$\frac{dL(t)}{dt} = \int_0^{L(t)} \frac{\partial v}{\partial x} dx. \quad (1)$$

81 Like others [3, 4, 22], we consider uniform growth conditions where  $\frac{\partial v}{\partial x}$  is independent of  
82 position, but potentially depends on time,  $t$ , so that we have  $\frac{\partial v}{\partial x} = \sigma(t)$ . Combining this  
83 definition with Equation (1) gives:

$$\frac{\partial v}{\partial x} = \sigma(t) = \frac{1}{L(t)} \frac{dL(t)}{dt}. \quad (2)$$

84 Without loss of generality, we assume that the domain elongates in the positive  $x$ -direction  
85 with the origin fixed, so that  $v(0, t) = 0$ . Integrating Equation (2) gives

$$v(x, t) = \frac{x}{L(t)} \frac{dL(t)}{dt}. \quad (3)$$

86 We now consider conservation of mass of some density function,  $C(x, t)$ , assuming that the  
87 population density function evolves according to a linear reaction–diffusion mechanism.  
88 The associated conservation statement on the growing domain can be written as

$$\frac{\partial C}{\partial t} = D \frac{\partial^2 C}{\partial x^2} - \frac{\partial(Cv)}{\partial x} + kC, \quad (4)$$

89 on  $0 \leq x \leq L(t)$ , where  $D > 0$  is the diffusivity,  $k$  is the production rate and  $v$  is  
90 the velocity associated with the underlying domain growth, given by Equation (3). We  
91 note that setting  $k > 0$  represents a source term which is relevant to ENS development  
92 since the precursor cells proliferate [16–18, 20]; however, our approach can also be used to  
93 study decay processes by setting  $k < 0$ .

94 To solve Equation (4) we must specify initial conditions and boundary conditions.  
95 Motivated by Landman et al. [22], we choose

$$C(x, 0) = \begin{cases} C_0 & 0 \leq x < \beta, \\ 0 & \beta \leq x \leq L(0), \end{cases} \quad (5)$$

96 which corresponds to some initial length of the domain,  $0 \leq x < \beta$ , being uniformly  
97 colonized at density  $C_0$ , and the remaining portion of the domain being uncolonized. We  
98 suppose that we have zero diffusive flux conditions at both boundaries,  $\frac{\partial C}{\partial x} = 0$  at  $x = 0$   
99 and  $x = L(t)$ , and we now seek to find an exact solution,  $C(x, t)$ .

## 100 2 Results

### 101 2.1 Exact solution

102 The first step in our solution strategy is to transform the spatial variable to a fixed domain,

103  $\xi = \frac{x}{L(t)}$  [3, 4, 10–12, 22], giving

$$\frac{\partial C}{\partial t} = \frac{D}{L^2(t)} \frac{\partial^2 C}{\partial \xi^2} - \frac{1}{L(t)} \frac{\partial(Cv)}{\partial \xi} + kC + \frac{\xi}{L(t)} \frac{dL(t)}{dt} \frac{\partial C}{\partial \xi}, \quad (6)$$

104 on  $0 \leq \xi \leq 1$ . Recalling that  $v = \frac{x}{L(t)} \frac{dL(t)}{dt} = \xi \frac{dL(t)}{dt}$ , we re-write Equation (6) as

$$\frac{\partial C}{\partial t} = \frac{D}{L^2(t)} \frac{\partial^2 C}{\partial \xi^2} + (k - \sigma(t))C, \quad (7)$$

105 where, in the transformed coordinates, the impact of domain growth manifests in two  
106 different ways:

- 107 1. the coefficient of the diffusive transport term is inversely proportional to  $L^2(t)$ , and  
108 hence decreases with time, and
- 109 2. the addition of a source term,  $-C\sigma(t)$ , represents dilution associated with the ex-  
110 panding domain.

111 Following Crank [23] we re-scale time,

$$T = \int_0^t \frac{D}{L^2(s)} ds, \quad (8)$$

112 giving

$$\frac{\partial C}{\partial T} = \frac{\partial^2 C}{\partial \xi^2} + \frac{L^2(t)(k - \sigma(t))}{D} C. \quad (9)$$

113 Equation (8) gives a relationship between the original time variable,  $t$ , and the transformed  
114 variable,  $T$ , which means that we can write Equation (9) as

$$\frac{\partial C}{\partial T} = \frac{\partial^2 C}{\partial \xi^2} + f(T)C, \quad (10)$$

115 whose solution, with zero diffusive flux conditions at both boundaries, can be obtained  
116 by applying separation of variables [23], giving

$$C(\xi, T) = \sum_{n=0}^{\infty} a_n \cos(n\pi\xi) \exp(-(n\pi)^2 T) \exp\left(\int_0^T f(T^*) dT^*\right), \quad (11)$$

117 where  $n \in \mathbb{N}^0$ . Our exact solution for  $C(\xi, T)$  can be re-written in terms of the original  
118 coordinates, giving  $C(x, t)$ . The Fourier coefficients,  $a_n$ , can be chosen to ensure that the  
119 exact solution satisfies the initial condition, given by Equation (5). Our framework for  
120 finding  $C(x, t)$  is quite general and does not depend on any particular form of the initial  
121 condition. We now present the details for a few relevant choices of  $L(t)$ .

### 122 2.1.1 Case 0: Non-growing domain

123 Before we present results for a growing domain it is instructive to consider the solution of  
124 Equation (4), with the same initial condition and boundary conditions, on a non-growing  
125 domain,  $0 \leq x \leq L$ . With  $L(t) = L$ , we have  $\sigma(t) = 0$  and  $T = \frac{Dt}{L^2}$ . Later, when  
126 we compare the solution of Equation (4) on a growing domain with the solution on a  
127 non-growing domain, it will be useful to recall that on a non-growing domain, as  $t \rightarrow \infty$ ,  
128 we have  $T \rightarrow \infty$ , since  $D > 0$  and  $L > 0$ . On the non-growing domain the solution of

129 Equation (4) can be written as

$$C(x, t) = \sum_{n=0}^{\infty} a_n \cos\left(\frac{n\pi x}{L}\right) \exp\left(-\frac{D(n\pi)^2 t}{L^2} + kt\right), \quad (12)$$

130 where  $a_0 = \frac{\beta C_0}{L}$ ,  $a_n = \frac{2C_0}{n\pi} \sin\left(\frac{n\pi\beta}{L}\right)$  and  $n \in \mathbb{N}^+$ .

### 131 2.1.2 Case 1: Exponential domain growth

132 With  $L(t) = L(0)\exp(\alpha t)$ , we have  $\sigma(t) = \alpha$  and  $T = D \left[ \frac{1 - \exp(-2\alpha t)}{2\alpha L(0)^2} \right]$ , for which we  
 133 note that as  $t \rightarrow \infty$ , we have  $T \rightarrow \frac{D}{2\alpha L(0)^2}$ , since  $\alpha > 0$ . This limiting behavior is different  
 134 to the limiting behavior under non-growing conditions. For an exponentially-elongating  
 135 domain, the solution of Equation (4) can be written as

$$C(x, t) = \sum_{n=0}^{\infty} a_n \cos\left(\frac{n\pi x}{L(t)}\right) \exp\left(-\frac{D(n\pi)^2 (1 - \exp(-2\alpha t))}{2\alpha L(0)^2} + t(k - \alpha)\right), \quad (13)$$

136 where  $a_0 = \frac{\beta C_0}{L(0)}$ ,  $a_n = \frac{2C_0}{n\pi} \sin\left(\frac{n\pi\beta}{L(0)}\right)$  and  $n \in \mathbb{N}^+$ .

### 137 2.1.3 Case 2: Linear domain growth

138 With  $L(t) = L(0) + bt$ , we have  $\sigma(t) = \frac{b}{L(t)}$  and  $T = \frac{Dt}{L(0)L(t)}$ , for which as  $t \rightarrow \infty$ , we  
 139 have  $T \rightarrow \frac{D}{bL(0)^2}$ , since  $D > 0$  and  $b > 0$ . For a linearly-elongating domain, the solution  
 140 of Equation (4) can be written as

$$C(x, t) = \sum_{n=0}^{\infty} a_n \frac{L(0)}{L(t)} \cos\left(\frac{n\pi x}{L(t)}\right) \exp\left(-\frac{(n\pi)^2 Dt}{L(0)L(t)} + \frac{kL(t)}{b}\right), \quad (14)$$

141 where  $a_0 = \frac{\beta C_0 \exp(-kL(0)/b)}{L(0)}$ ,  $a_n = \frac{2C_0 \exp(-kL(0)/b)}{n\pi} \sin\left(\frac{n\pi\beta}{L(0)}\right)$  and  $n \in \mathbb{N}^+$ .



## 142 2.2 Comparison of exact and numerical solutions

143 We now examine predictions made of our exact solution by comparing plots of  $C(x, t)$ ,  
144 generated using our exact solution, with plots of  $C(x, t)$ , generated using appropriate nu-  
145 merical approximations. To generate the numerical approximations we discretise Equa-  
146 tion (7) using a central finite difference approximation on a uniformly discretized domain,  
147  $0 \leq \xi \leq 1$ , with uniform mesh spacing  $\delta\xi$ . The resulting system of coupled ordinary dif-  
148 ferential equations is integrated through time using a backward Euler approximation with  
149 uniform time steps of duration  $\delta t$ . At each time step the resulting system of tridiagonal  
150 linear equations is solved using the Thomas algorithm [24]. All numerical results presented  
151 correspond to choices of  $\delta\xi$  and  $\delta t$  such that the numerical results are grid-independent.

152 Results in Fig. 1A–C compare exact and numerical solutions on an exponentially-  
153 growing domain at  $t = 0, 10$  and  $20$ , and we see that the exact and numerical solu-  
154 tions are indistinguishable. A summary of the properties of the solutions in the interval  
155  $0 \leq t \leq 20$  is given in a space-time diagram in Fig. 1D, which compares the length  
156 of the domain,  $L(t)$ , and the position of the front,  $f(t)$ . Here, we define the position  
157 of the front to be the spatial location where  $C(x, t) = 0.01$ . This means that we have  
158  $f(0) = \beta$ . Comparing  $L(t)$  and  $f(t)$  in Fig. 1D indicates that the  $C(x, t)$  profile moves  
159 in the positive  $x$ -direction as time increases; however, the distance between  $L(t)$  and  $f(t)$   
160 increases with time such that the  $C(x, t)$  profile does not colonize the domain by  $t = 20$ .

161 Results in Fig. 1E–G correspond to the same initial condition and parameters used in  
162 Fig. 1A–C except that we increased the diffusivity,  $D$ . Comparing results in Fig. 1E–G  
163 with the solutions in Fig. 1A–C indicates that the front moves faster with an increase  
164 in  $D$ , as we might anticipate. However, the summary of the time evolution of  $L(t)$  and  
165  $f(t)$  in Fig. 1H confirms that the increase in  $D$  is insufficient for colonization to occur by  
166  $t = 20$ . In contrast, the results in Fig. 1I–K correspond to the same initial condition and

167 parameters as in Fig. 1E–G except that we have further increased  $D$ . This time we see  
168 that the front catches up with  $L(t)$ , and we have full colonization by  $t = 20$ .

169 To further explore the competition between various processes in the model we compare  
170 some additional exact and numerical solutions in Fig. 2, where again we see that in all  
171 cases considered, the numerical solutions are visually indistinguishable from the exact  
172 solutions. The set of results in Fig. 2A–D is identical to the set of results shown previously  
173 in Fig. 1E–H, which corresponds to a case where the domain does not become fully  
174 colonized within the interval  $0 \leq t \leq 20$ . We also present a second set of results, in  
175 Fig. 2E–H, which are identical to those in Fig. 2A–D except for a change in the initial  
176 condition. We note that the initial condition in Fig. 2A–D corresponds to  $C(x, 0) = 1$   
177 for  $0 \leq x < 0.2$  and  $C(x, 0) = 0$  for  $0.2 \leq x \leq 1$ , whereas the initial condition in Fig.  
178 2E–H corresponds to  $C(x, 0) = 1$  for  $0 \leq x < 0.75$  and  $C(x, 0) = 0$  for  $0.75 \leq x \leq 1$ . The  
179 situation in Fig. 2A–D leads to unsuccessful colonization by  $t = 20$  whereas the scenario  
180 in Fig. 2E–H leads to successful colonization by  $t = 20$ . Therefore, these results are  
181 consistent with Landman et al.’s [22] numerical simulations which suggest that the initial  
182 condition plays a key role in determining whether or not colonization occurs.

183 Although all results presented in Fig. 1 and Fig. 2 correspond to an exponentially-  
184 growing domain, we also generated exact and numerical results for a linearly elongating  
185 domain (not shown), and we note two key outcomes. First, similar to the results in Fig.  
186 1 and Fig. 2, we found that the exact solution and the numerical solutions compare very  
187 well. Second, we found that altering the initial condition,  $D$ ,  $k$  and the growth rate,  $b$ ,  
188 could affect whether or not the system colonized within a specified time interval.

## 189 2.3 Criteria for colonization

190 Now that we have derived and validated exact solutions describing a linear reaction–  
191 diffusion process on a growing domain we can use the new solution to write down a  
192 condition which can be used to distinguish between situations which lead to successful  
193 colonization from situations which lead to unsuccessful colonization. For our initial con-  
194 dition, given by Equation (5), we aim to identify whether the spreading density profile,  
195  $C(x, t)$ , ever reaches the boundary,  $x = L(t)$ , by some threshold time  $t^\star$ . To explore  
196 this we must examine the quantity  $C(L(t^\star), t^\star)$  by substituting  $x = L(t^\star)$  and  $t = t^\star$   
197 into Equation (11). Having evaluated this quantity, we test whether  $C(L(t^\star), t^\star) > \varepsilon$ , in  
198 which case we have successful colonization by time  $t^\star$ . Alternatively, if  $C(L(t^\star), t^\star) < \varepsilon$ ,  
199 we have unsuccessful colonization by time  $t^\star$ . Here  $\varepsilon$  is some user-defined small tolerance.  
200 For example, to interpret the results in Fig. 1 and Fig. 2, we set  $\varepsilon = 0.01$  to determine  
201 the position of the front, and this choice of  $\varepsilon$  could be used to make a distinction between  
202 successful and unsuccessful colonization in other applications.

## 203 3 Discussion and Conclusions

204 In this work we derive and validate an exact solution for a linear reaction–diffusion PDE on  
205 a uniformly growing domain. Our framework is relevant for a general class of uniformly  
206 growing domains,  $0 \leq x \leq L(t)$ , and we present specific results for exponentially-  
207 elongating domains,  $L(t) = L(0)\exp(\alpha t)$ , with  $\alpha > 0$ , and linearly-elongating domains,  
208  $L(t) = L(0) + bt$ , with  $b > 0$ . While our approach is relevant for a general class of initial  
209 conditions, motivated by Landman et al.’s previous work [22], we consider an initial  
210 condition relevant to ENS development where we consider  $C(x, 0)$  to be localised near  
211 one boundary of the domain. Then, using our exact solution, we explore whether the

212 density profile evolves such that it can overcome the domain growth and colonize the  
213 entire length of the domain by reaching the other boundary, within some particular time  
214 interval.

215 It is interesting to note, and discuss, several differences between the solution of the  
216 linear reaction–diffusion PDE on a non-growing domain, given by Equation (12), and the  
217 solutions of the same PDE on a growing domain, such as Equations (13) and (14). In  
218 the usual way, the solution on a non-growing domain (Equation (12)) indicates that after  
219 a sufficiently long period of time the exact solution can be approximated by the first  
220 few terms in the infinite series since the factor  $\exp\left(-\frac{D(n\pi)^2t}{L^2}\right)$  guarantees that further  
221 terms in the series decrease exponentially fast with time. On a non-growing domain, this  
222 could be used to develop useful approximations to Equation (12), such as

$$C(x, t) \approx \frac{\beta}{L(0)} \exp(kt) + \frac{2}{\pi} \sin\left(\frac{\pi\beta}{L}\right) \cos\left(\frac{\pi x}{L}\right) \exp\left(-\frac{D\pi^2 t}{L^2} + kt\right). \quad (15)$$

223 Such approximations are well-known to be accurate after a sufficiently long period of  
224 time [25,26]. One of the key differences between the solutions of Equation (4) on a grow-  
225 ing and non-growing domain becomes obvious when we consider whether it is possible to  
226 develop a useful approximation of the exact solution in the long-time limit on a growing  
227 domain. Since Equation (11) contains the factor  $\exp(-(n\pi)^2T)$ , it is tempting to think  
228 that we may truncate the infinite series after one or two terms to obtain a useful approx-  
229 imation to the exact solution when  $T$  becomes sufficiently large. This kind of approxi-  
230 mation is possible in the non-growing case where, as we previously noted, when  $t \rightarrow \infty$ ,  
231 we have  $T \rightarrow \infty$ . However, different behavior occurs in the growing domain solutions.  
232 In particular, for the exponentially-growing domain, as  $t \rightarrow \infty$  we have  $T \rightarrow \frac{D}{2\alpha L(0)^2}$ .  
233 Similarly, in the linearly-growing domain case, as  $t \rightarrow \infty$  we have  $T \rightarrow \frac{D}{bL(0)^2}$ . This

234 means that it may not be possible to develop simple approximations for sufficiently large  
235  $t$ . Indeed, we explored whether it is possible to approximate the exact solutions in Fig. 1  
236 and Fig. 2 using a two-term truncation of Equation (13) and we found that this produced  
237 a very poor approximation, even for much larger values of  $t$  than reported here, such as  
238  $t = 100$ .

239 Since we rely on separation of variables and superposition to construct our exact  
240 solution, one of the key limitations of our strategy is that the exact solution applies only to  
241 a linear reaction–diffusion process. While many reaction–diffusion models are inherently  
242 nonlinear, there is a real practical value in the use of linear models, since linear PDE  
243 models are often used to approximate the solution of related nonlinear PDE models. For  
244 example, Hickson et al. [27] analyses the critical timescale of a nonlinear reaction-diffusion  
245 process by arguing that the nonlinear PDE model can be approximated by a linear PDE  
246 model. Similarly, Swanson [28] provides key insight into the motion of a moving front  
247 of cells by studying an exact solution of a linear PDE model. In this case, Swanson [28]  
248 assumes that the linear PDE model can be used to approximate the solution of a nonlinear  
249 PDE. Using a similar approach, Witelski [29] studies the motion of wetting fronts in  
250 variably saturated porous media, which is governed by a nonlinear PDE, by first analysing  
251 the solution a related linear PDE model. These kinds of approximations are invoked  
252 in many other situations such as the study of flow in saturated porous media [30, 31],  
253 solid-liquid separation processes [32], and certain problems in food manufacturing [33].  
254 Therefore, while our exact solution cannot be applied directly to study the solution of  
255 nonlinear PDE models, the basic properties of the linear PDE model can be used to  
256 provide insight into reaction–diffusion processes on a growing domain. In addition to this  
257 practical value, we believe that our exact solution is also inherently interesting from a  
258 mathematical point of view.

259 There are several ways in which the exact solution strategy presented in this work  
260 could be extended. Although we have only considered a single species reaction–diffusion  
261 processes where we have one dependent variable,  $C(x, t)$ , in principle our solution strat-  
262 egy could also be applied to multispecies reaction–diffusion processes involving several  
263 dependent variables,  $C_1(x, t), C_2(x, t), C_3(x, t), \dots$ , that are coupled through a linear re-  
264 action network [34]. We anticipate that these kinds of multispecies problems could be  
265 solved exactly on a uniformly growing domain by first applying a linear transformation  
266 which uncouples the reaction network [34]. After this initial uncoupling transformation,  
267 our solution strategy could be applied to solve each uncoupled PDE before applying the  
268 inverse uncoupling transform to give an exact solution for the coupled multispecies PDE  
269 problem on a growing domain. We leave this extension for future consideration.

## 270 **Acknowledgments**

271 I acknowledge the support from the Australian Research Council (FT130100148) and am  
272 grateful for the advice and assistance of Emeritus Professor Sean McElwain and Associate  
273 Professor Scott McCue.

## 274 **References**

- 275 1. Wolpert L (2011) Principles of Development. 4th Edition. Oxford. Oxford Univer-  
276 sity Press.
- 277 2. Meinhardt H (1982) Models of biological pattern formation. London. Academic  
278 Press.
- 279 3. Crampin EJ, Gaffney EA, Maini PK (1999) Reaction and diffusion on growing  
280 domains: scenarios for robust pattern formation. Bull Math Biol. 61: 1093–1120.
- 281 4. Crampin EJ, Hackborn WW, Maini PK (2002) Pattern formation in reaction-  
282 diffusion models with nonuniform domain growth. Bull Math Biol. 64: 747–769.
- 283 5. Kondo S, Asai R (1995) A reaction-diffusion wave on the skin of the marine angelfish  
284 pomacanthus. Nature. 376: 765–768.
- 285 6. Painter KJ, Maini PK, Othmer HG (1997) Stripe formation in juvenile pomacan-  
286 thus explained by a generalized Turing mechanism with chemotaxis. PNAS. 96:  
287 5549–5554.
- 288 7. Murray JD (2002) Mathematical Biology. 2nd Edition. New York. Springer.
- 289 8. Chisholm RH, Hughes BD, Landman KA (2010) Building a morphogen gradient  
290 without diffusion in a growing tissue. PLoS ONE. 5(9): e12857.
- 291 9. Thompson RA, Yates CA, Baker RE (2012) Modelling cell migration and adhesion  
292 during development. Bull Math Biol. 74: 2793–2809.
- 293 10. Baker RE, Yates CA, Erban R (2009) From microscopic to macroscopic descriptions  
294 of cell migration on growing domains. Bull Math Biol. 72(3): 719–762.

- 295 11. Yates CA, Baker RE, Erban R, Maini PK (2012) Going from microscopic to macro-  
296 scopic on nonuniform growing domains. *Phys Rev E*. 86: 021921.
- 297 12. Yates CA (2014) Discrete and continuous models for tissue growth and shrinkage.  
298 *J Theor Biol*. 350: 37–48.
- 299 13. Binder BJ, Landman KA (2009) Exclusion processes on a growing domain. *J Theor*  
300 *Biol*. 259: 541–551.
- 301 14. Hywood JD, Landman KA (2013) Biased random walks, partial differential equa-  
302 tions and update schemes. *ANZIAM J*. 55: 93–108.
- 303 15. Le Douarin NM, Teillet MA (1973) The migration of neural crest cells to the wall  
304 of the digestive tract in avian embryo. *J Embryol Exp Morphol*. 30: 31–48.
- 305 16. Newgreen DF, Erikson CA (1986) The migration of neural crest cells. *Int Rev Cytol*.  
306 103: 89–145.
- 307 17. Newgreen DF, Southwell B, Hartley L, Allan IJ (1996) Migration of enteric neural  
308 crest cells in relation to growth of the gut in avian embryos. *Acta Anat*. 157: 105–  
309 115.
- 310 18. Kulesa PM, Fraser SE (1998) Neural crest cell dynamics revealed by time-lapse  
311 video microscopy of whole embryo chick explant cultures. *Dev Biol*. 204: 327–344.
- 312 19. Gershon MD, Ratcliffe EM (2004) Developmental biology of the enteric nervous  
313 system: Pathogenesis of Hirschsprung’s disease and other congenital dysmotilities.  
314 *Semin Pediatr Surg*. 13(4): 224–235.



- 315 20. Newgreen DF, Dufour S, Howard MJ, Landman KA (2013) Simple rules for a  
316 “simple” nervous system? Molecular and biomathematical approaches to enteric  
317 nervous system formation and malformation. *Dev Biol.* 382: 305–319.
- 318 21. Young HM, Bergner AJ, Simpson MJ, KcKeown SJ, Hao MM, Anderson CR,  
319 Enomoto H (2014) Colonizing while migrating: how do individual enteric neural  
320 crest cells behave? *BMC Biol.* 12: 23.
- 321 22. Landman KA, Pettet GJ, Newgreen DF (2003) Mathematical models of cell colo-  
322 nization of uniformly growing domains. *Bull Math Biol.* 65: 235–262.
- 323 23. Crank J (1975) *The mathematics of diffusion.* 2nd Edition. Oxford. Oxford Univer-  
324 sity Press.
- 325 24. Simpson MJ, Landman KA, Newgreen DF (2006) Chemotactic and diffusive mi-  
326 gration on a nonuniformly growing domain: numerical algorithm development and  
327 applications. *J Comp Appl Math.* 192: 282–300.
- 328 25. Farlow SJ (1982) *Partial differential equations for scientists and engineers.* New  
329 York. Dover.
- 330 26. Haberman R (2004) *Applied partial differential equations: With Fourier series and*  
331 *boundary value problems.* New York, Prentice Hall.
- 332 27. Hickson RI, Barry SI, Sidhu HS, Mercer GN (2011) Critical times in single layer  
333 reaction diffusion. *Int J Heat Mass Transf.* 54: 2642–2650.
- 334 28. Swanson KR (2008) Quantifying glioma cell growth and invasion in vitro. *Math*  
335 *Comput Model.* 47: 638–648.

- 336 29. Witelski TP (2005) Motion of wetting fronts moving into partially pre-wet soil. Adv  
337 Water Resour. 28: 1133–1141.
- 338 30. Simpson MJ, Jazaei F, Clement TP (2013) How long does it take for aquifer recharge  
339 or aquifer discharge processes to reach steady state? J Hydrol. 501: 241–248.
- 340 31. Jazaei F, Simpson MJ, Clement TP (2014) An analytical framework for quantify-  
341 ing aquifer response time scales associated with transient boundary conditions. J  
342 Hydrol. 519: 1642–1648.
- 343 32. Landman KA, White LR (1997) Predicting filtration time and maximizing through-  
344 put in a pressure filter. AIChE Journal. 43: 3147–3160.
- 345 33. Landman KA, McGuinness MJ (2000) Mean action time for diffusive processes. J  
346 Appl Math Decision Sci. 4: 125–141.
- 347 34. Sun Y, Clement TP (1999) A decomposition method for solving coupled multi-  
348 species reactive transport equations. Transport Porous Med. 37: 327–346.

## <sup>349</sup> Figure Legends

350 **Figure 1: Comparison of exact and numerical solutions, exploring the influence**  
351 **of varying the diffusivity,  $D$ .** All results correspond to an exponentially-elongating  
352 domain,  $L(t) = L(0)\exp(\alpha t)$ , with  $L(0) = 1$  and  $\alpha = 0.1$ . The initial condition is given by  
353 Equation (5) with  $\beta = 0.2$  and  $C_0 = 1$ . In all cases we consider a linear source term with  
354  $k = 0.105$ . Results in (a)–(d) correspond to  $D = 0.00001$ , results in (e)–(h) correspond to  
355  $D = 0.001$ , and results in (i)–(l) correspond to  $D = 0.01$ . For all three sets of parameter  
356 combinations we show the solution at  $t = 0, 10$  and  $t = 20$ , as indicated. The exact solu-  
357 tions, presented in (a)–(c), (e)–(g) and (i)–(k) (solid blue), correspond to Equation (13),  
358 where we truncate the infinite sum after 1000 terms. The numerical solutions, presented  
359 in (a)–(c), (e)–(g) and (i)–(k) (dashed red), are numerical approximations of Equation  
360 (7) with  $\delta\xi = 0.001$  and  $\delta t = 0.001$ . The space–time diagrams summarising the time  
361 evolution of the length of the domain,  $L(t)$ , and the position of the front of the  $C(x, t)$   
362 density profile,  $f(t)$ , given in (d), (h) and (l), are constructed by defining  $f(t)$  to be the  
363 position where  $C(x, t) = 0.01$ .

364

365 **Figure 2: Comparison of exact solutions and numerical approximations, explor-**  
366 **ing the influence of varying the width of the initial condition,  $\beta$ .** All results  
367 correspond to an exponentially-elongating domain,  $L(t) = L(0)\exp(\alpha t)$ , with  $L(0) = 1$   
368 and  $\alpha = 0.1$ . The initial condition is given by Equation (5) with  $C_0 = 1$ , and in all  
369 cases we set  $k = 0.105$  and  $D = 0.001$ . Results in (a)–(d) correspond to a narrow ini-  
370 tial condition,  $\beta = 0.2$ , whereas results in (e)–(h) correspond to a wide initial condition,  
371  $\beta = 0.75$ . For both sets of results we show the solution at  $t = 0, 10$  and  $t = 20$ , as  
372 indicated. The exact solutions, presented in (a)–(c) and (e)–(g) (solid blue), correspond  
373 to Equation (13), where we truncate the infinite sum after 1000 terms. The numerical  
374 solutions, presented in (a)–(c) and (e)–(g) (dashed red), correspond to are numerical ap-  
375 proximations of Equation (7) with  $\delta\xi = 0.001$  and  $\delta t = 0.001$ . The space–time diagrams  
376 summarising the time evolution of the length of the domain,  $L(t)$ , and the position of the  
377 front of the  $C(x, t)$  density profile,  $f(t)$ , given in (d) and (h), are constructed by defining  
378  $f(t)$  to be the position where  $C(x, t) = 0.01$ .

379

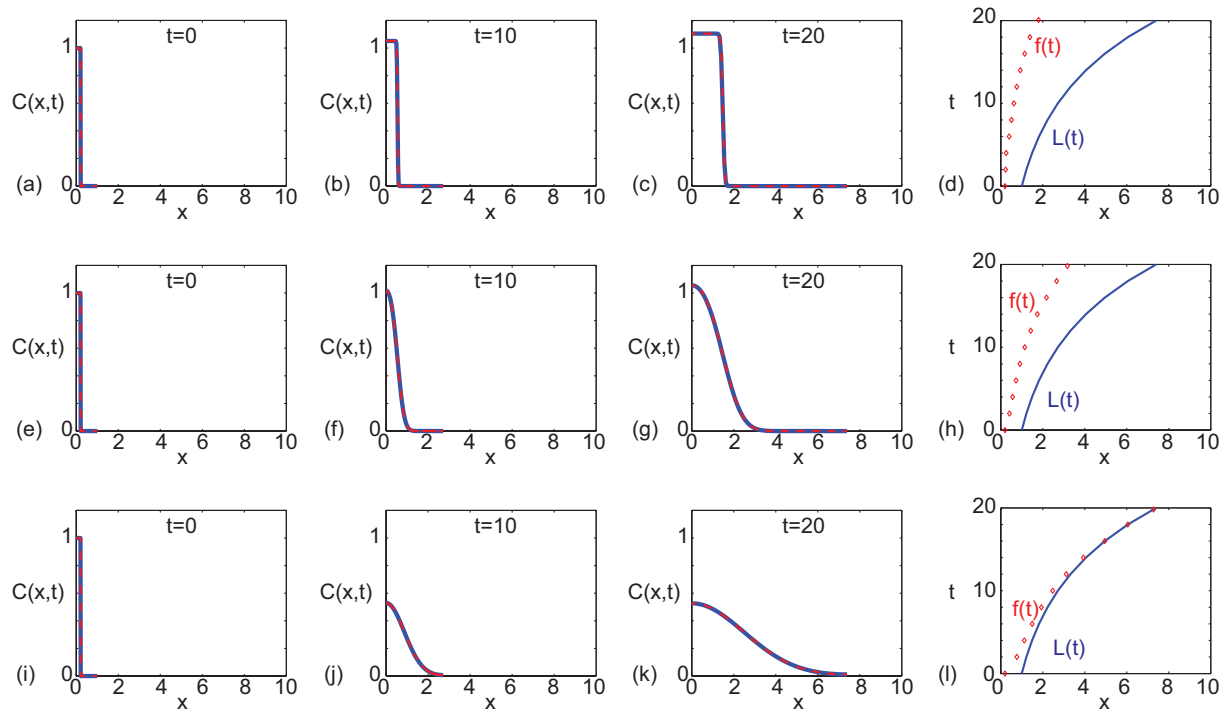


Figure 1:

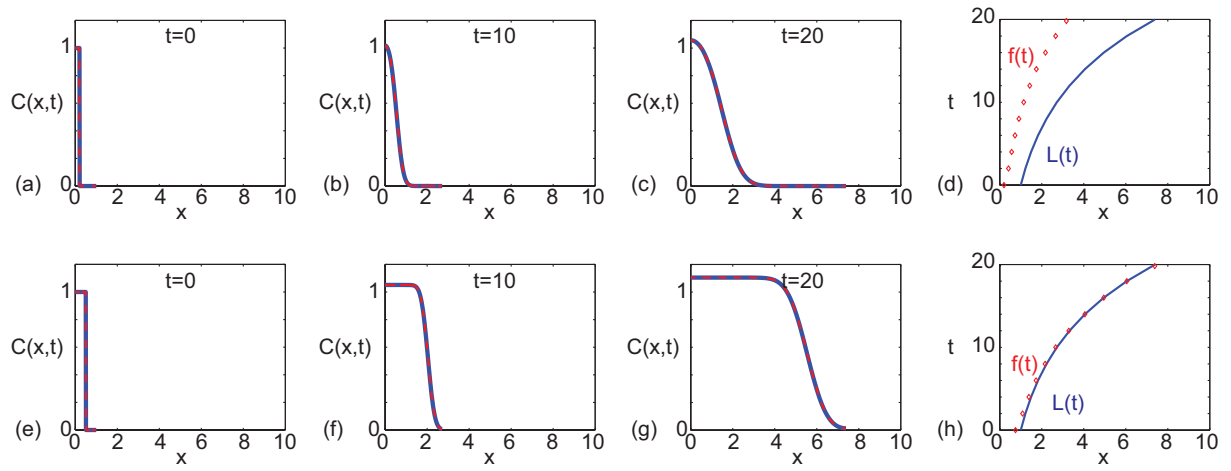


Figure 2: